Composite fading in non-line-of-sight off-body communications channels

Yoo, SK & Cotton, S

DOI 10.23919/eucap.2017.7928458

Publisher: IEEE

Composite Fading in Non-line-of-Sight Off-Body Communications Channels

Seong Ki Yoo and Simon L. Cotton
Institute of Electronics, Communication & Information Technology
Queen's University Belfast, BT3 9DT, UK
{syoo02, simon.cotton}@qub.ac.uk

***Abstract*—In this paper, we investigate the characteristics of the composite fading observed in non-line-of-sight (NLOS) off-body communications channels using the η-μ/inverse gamma distribution. We use a number of different datasets obtained from NLOS off-body measurements which have been performed in a range of different environments at 5.8 GHz and 60 GHz. In all cases, the bodyworn node was positioned on the front-central chest region of an adult male. It is shown that the η-μ/inverse gamma model provides an excellent fit to the measurement data for all of the considered cases. Using the Akaike information criterion (AIC), we have compared the η-μ/inverse gamma model with other composite and non-composite fading models associated with the NLOS channel conditions. The AIC results confirm that the η-μ/inverse gamma model was the most likely model to have been responsible for generating the channel data from the set of candidates which were considered.**

***Index Terms*—composite fading, η-μ/inverse gamma distribution, off-body channel, non-line-of-sight channel.**

I. Introduction

To take into account the simultaneous effect of multipath and shadowing, a number of studies have proposed the use of composite fading models for both conventional and emerging communications channels [1–4]. Among the emergent communications channels are those found in body-centric applications, which have gained much attention in the literature due to the wide range of potential use cases in the sports, medical, military and entertainment sectors.

As a result, new composite fading models have been proposed and used to model body centric communications channels [5–8]. For example, in [5], the composite fading experienced in on-, off- and body-to-body channels was characterized using the κ-μ/lognormal distribution which assumes that the resultant dominant signal component is shadowed and follows the lognormal distribution. In contrast, the authors of [6] have extensively characterized the composite fading observed in indoor off-body channels using the κ-μ/gamma distribution which assumes that the mean signal power of the multipath components, i.e. both the dominant and scattered components, undergoes shadowing and follows the gamma distribution. More recently, the authors of [7], [8] have proposed two new composite fading models based on the κ-μ and η-μ distributions respectively. These new models have many advantages over the composite models proposed in [5], [6], not least that they are extremely tractable and their primary statistics of interest can be expressed in convenient closed-form expressions.

In off-body communications systems, at least one end of the communications link is positioned on the human body. Consequently, the overall system performance can suffer from complex antenna-body interaction effects such as radiation pattern distortion and reduced radiation efficiency [9]. Additionally, due to the transceiver operating in close proximity to the human body, the wireless link can be prone to shadowing events induced by the movement of body parts and blockages caused by both the user's body and/or surrounding people and obstacles [10]. The net result of all of these factors may be deep fades in the received signal which can degrade the overall signal reliability.

Quite often in off-body communications channels, there may exist no direct signal path between the transmitter (Tx) and receiver (Rx). This may happen for example when the user's body obstructs the optical line of sight path between the Tx and Rx. In this instance, it is more reasonable to assume that scattered multipath components exist only, i.e. the off-body link is supported by non-line-of-sight (NLOS) channel conditions, and its mean power is subject to shadowing effect which be induced by the user's body or the local surroundings (or a combination of both). Therefore, in this study, we investigate the characteristics of the composite fading observed in NLOS off-body channels using the η-μ/inverse gamma distribution proposed in [8]. Furthermore, we compare our results with the Rayleigh, Nakagami-m and Nakagami/gamma [4] models which are traditionally associated with NLOS channel conditions.

This paper is organized as follows. Section II briefly introduces the η-μ/inverse gamma fading model. Section III describes the 5.8 GHz and 60 GHz NLOS off-body channel measurement set-up, environments and scenarios. In Section IV, the parameter estimates and model fitting are presented along with the model selection. Finally, Section V concludes the paper with some closing remarks.

II. Composite Fading Model

The probability density function (PDF) of the composite signal envelope, R, in an η-μ/inverse gamma fading channel can be expressed as shown in (1) at the top of the next page [8]. In (1), $\Gamma(\cdot)$ and ${}_2F_1(\cdot,\cdot;\cdot;\cdot)$ represent the gamma

$$f_R(r) = \frac{4\sqrt{\pi}\,\mu^{2\mu}\,h^{\mu}\beta^{\alpha}r^{4\mu-1}\Gamma(\alpha+2\beta)}{(2\mu hr^2+\beta)^{\alpha+2\beta}\Gamma(\mu)\,\Gamma(\alpha)\,\Gamma\left(\mu+\frac{1}{2}\right)}\,{}_2F_1\left(\frac{\alpha+2\beta}{2},\,\frac{\alpha+2\beta+1}{2}\;;\;\mu+\frac{1}{2}\;;\left(\frac{2\mu Hr^2}{2\mu hr^2+\beta}\right)^2\right) \tag{1}$$

and Gaussian hypergeometric functions respectively. In terms of its physical interpretation, η is defined as the scattered wave power ratio between the in-phase and quadrature components of each cluster of multipath in *Format* 1 whereas the correlation coefficient between the scattered wave in-phase and quadrature components of each cluster of multipath in *Format* 2 [11]. It is worth noting that *Format* 1 is utilized in this study and thus $h = \frac{2+\eta^{-1}+\eta}{4}$ and $H = \frac{\eta^{-1}+\eta}{4}$in (1). The μ parameter is related to the number of multipath clusters while α and β are the shape and scale parameters of the inverse gamma distribution. In (1), the α parameter controls the amount of the shadowing of the mean signal power. More specifically, as α approaches infinity (i.e. $\alpha \to \infty$), there is no shadowing and thus the mean signal power becomes deterministic. Accordingly, the PDF given in (1) corresponds to the η-μ PDF. On the other hand, as α approaches zero (i.e. $\alpha \to 0$), the scattered signal components are completely shadowed.

III. Channel Measurements

A. 5.8 GHz NLOS off-body measurements

The 5.8 GHz NLOS off-body channel measurements were performed within three indoor environments, namely a laboratory room, a seminar room and an open office area. These are spread over the 1st or 2nd floors of the Institute of Electronics, Communications and Information Technology (ECIT) at Queen's University Belfast in the United Kingdom. The details of the environments are described in [6]. The Tx used for the 5.8 GHz NLOS off-body measurements consisted of an ML 5805 transceiver manufactured by RFMD which was configured to generate a continuous wave signal with an output power of +17.6 dBm at 5.8 GHz. The Tx was situated tangentially with respect to the body surface of the front-central chest region of an adult male of height 1.83 m and mass 73 kg using a small strip of Velcro®. The measured free space and bodyworn azimuthal radiation patterns are presented in Fig. 1.

For the Rx, a single antenna was positioned on a non-conductive polyvinyl chloride (PVC) pole at height of 1.10 m above the floor level so that it was vertically polarized. It was connected to port 1 of a Rohde & Schwarz ZVB-8 vector network analyzer (VNA) using a low-loss coaxial cable. The VNA setup was configured as a sampling receiver, recording the b_1 wave quantity incident on port 1 with a bandwidth of 10 kHz and a channel sample rate of 425.6 Hz. The antennas used by both the Tx and Rx were omnidirectional sleeve dipole antennas with +2.3 dBi gain (Mobile Mark model PSKN3-24/55S) in free space. For the NLOS off-body channel conditions, the test subject walked away from the Rx in a straight line (from 1 m point to 9 m point) for each environment.

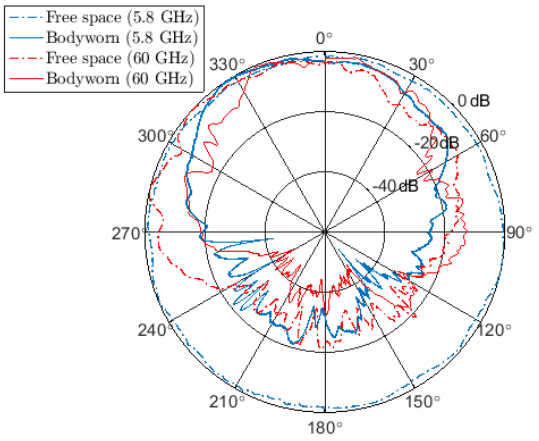

Fig. 1. The measured free space and bodyworn azimuthal radiation patterns at 5.8 GHz and 60 GHz.

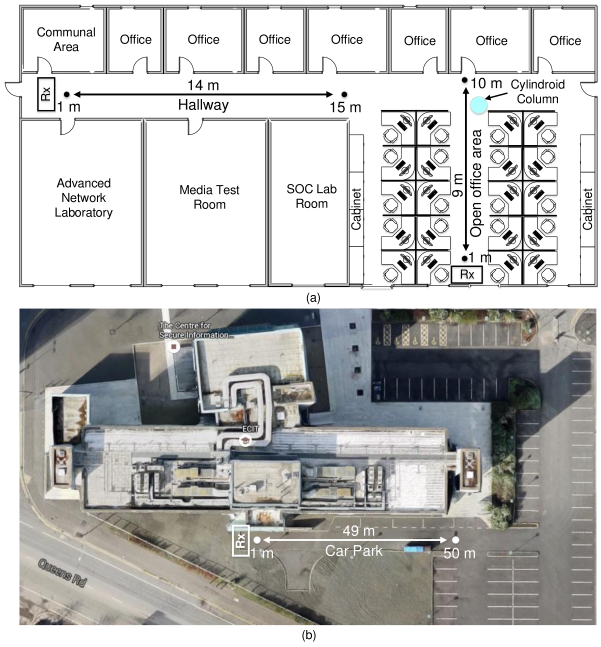

Fig. 2. 60 GHz NLOS off-body channel measurement environments: (a) indoor hallway and open office area; (b) outdoor car park.

B. 60 GHz NLOS off-body measurements

The 60 GHz NLOS off-body channel measurements were conducted within four different environments, namely a hallway, an open office, an anechoic chamber and a car park. The hallway and open office environments are located on the 1st floor of the ECIT building. As shown in Fig. 2, the open

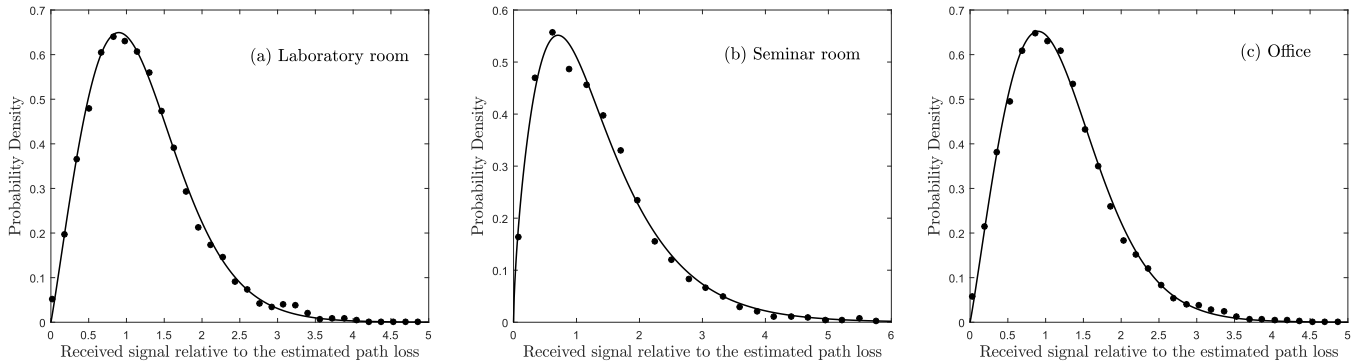

Fig. 3. Empirical PDFs (symbols) of the composite fading observed in the NLOS off-body channel at 5.8 GHz within (a) the laboratory room, (b) the seminar room and (c) the open office area environments compared to the theoretical PDFs for the η-μ/inverse gamma (continuous lines) model.

office area contained a number of soft partitions, cabinets, PCs, chairs and desks. The anechoic chamber is described in [12] and outdoor car park is adjacent to the ECIT building.

The 60 GHz off-body measurement system consist of a Hittite HMC6000LP711E Tx and Hittite HMC6001LP711E Rx modules. Both the Tx and Rx modules contain on-chip low profile antennas with +7.5 dBi gain. The Tx was configured to generate a continuous wave signal at the maximum Equivalent Isotropically Radiated Power (EIRP) of +21.1 dBm[1] and was securely fixed to the inside of a compact acrylonitrile butadiene styrene (ABS) enclosure (80 mm × 80 mm × 20 mm). During the measurements, the Tx was positioned on the front-central chest region of an adult male of height of 1.83 m and mass 78 kg using a small strip of Velcro®. The measured azimuthal radiation patterns for the Tx antenna in free space and positioned on the front-central chest region of the human body are also shown in Fig. 1. The Rx was positioned on a non-conductive polyvinyl chloride (PVC) stand at an elevation of 2.38 m above the floor level so that the Rx antenna was vertically polarized. The complex baseband output of the Rx module was connected to port 1 of a Rhode & Schwarz ZVB-8 VNA using an I/Q differential splitter network and SubMiniature version A (SMA) barrel connectors. The setup was configured to record the b_1 wave quantity incident on port 1 with a bandwidth of 100 kHz and a channel sample rate of 118 Hz.

Similar to the 5.8 GHz NLOS off-body measurements, the test subject walked away from the Rx in a straight line for the NLOS off-body channel conditions. Due to the dissimilar size of each environment, the walking distances for each environment were different, in particular, hallway (14 m), open office (9 m), anechoic chamber (7 m) and car park (49 m). It is worth highlighting that only first 5 m of the off-body channel data in the car park environment was used in data analysis due to the received signal power regularly extending below the noise threshold of the receiver beyond this point.

[1]The EIRP was measured in a non-reverberant setting at a separation distance of 0.24 m using a Keysight E8361C Network Analyzer and a 20 dB gain horn antenna manufactured by Flann (model no. 25240-25).

TABLE I
PARAMETER ESTIMATES OF THE η-μ/INVERSE GAMMA FADING MODEL FOR ALL OF THE CONSIDERED NLOS OFF-BODY MEASUREMENT DATA.

Frequency	Environments	η	μ	α	β
5.8 GHz	Laboratory	1.00	0.52	8.92	14.69
	Seminar	0.21	0.41	5.40	11.74
	Open office	1.00	0.52	9.04	14.84
60 GHz	Hallway	0.04	0.95	20.00	32.67
	Open office	5.89	0.79	3.56	4.96
	Anechoic	5.33	0.87	14.87	21.54
	Car park	1.00	1.25	2.90	3.01

IV. RESULTS

A. Data fitting

For both frequency bands, the composite fading signal was first abstracted by removing the estimated path loss from the raw measurement data using the log-distance path loss given in [13]. Then the corresponding parameter estimates for the η-μ/inverse gamma model were obtained using a non-linear least squares routine programmed in MATLAB to fit (1) to the NLOS off-body measurement data. As an example of data fitting process, Figs. 3 and 4 show the empirical PDFs and theoretical PDFs of the η-μ/inverse gamma fading model for all of the 5.8 GHz and 60 GHz NLOS off-body measurement data, respectively. It is obvious that the η-μ/inverse gamma fading model provided an excellent fit to the NLOS off-body measurement data for all of the considered cases in this study. Table I provides the parameter estimates for the η-μ/inverse gamma fading model for all of the measurement data. This allows the reader to reproduce their own simulated composite fading data.

Interestingly, for the 5.8 GHz frequency band, the parameter estimates obtained for the laboratory environment were quite similar to those for the open office environment, suggesting that similar composite fading was experienced in both environments. It was also observed that the scattered wave power

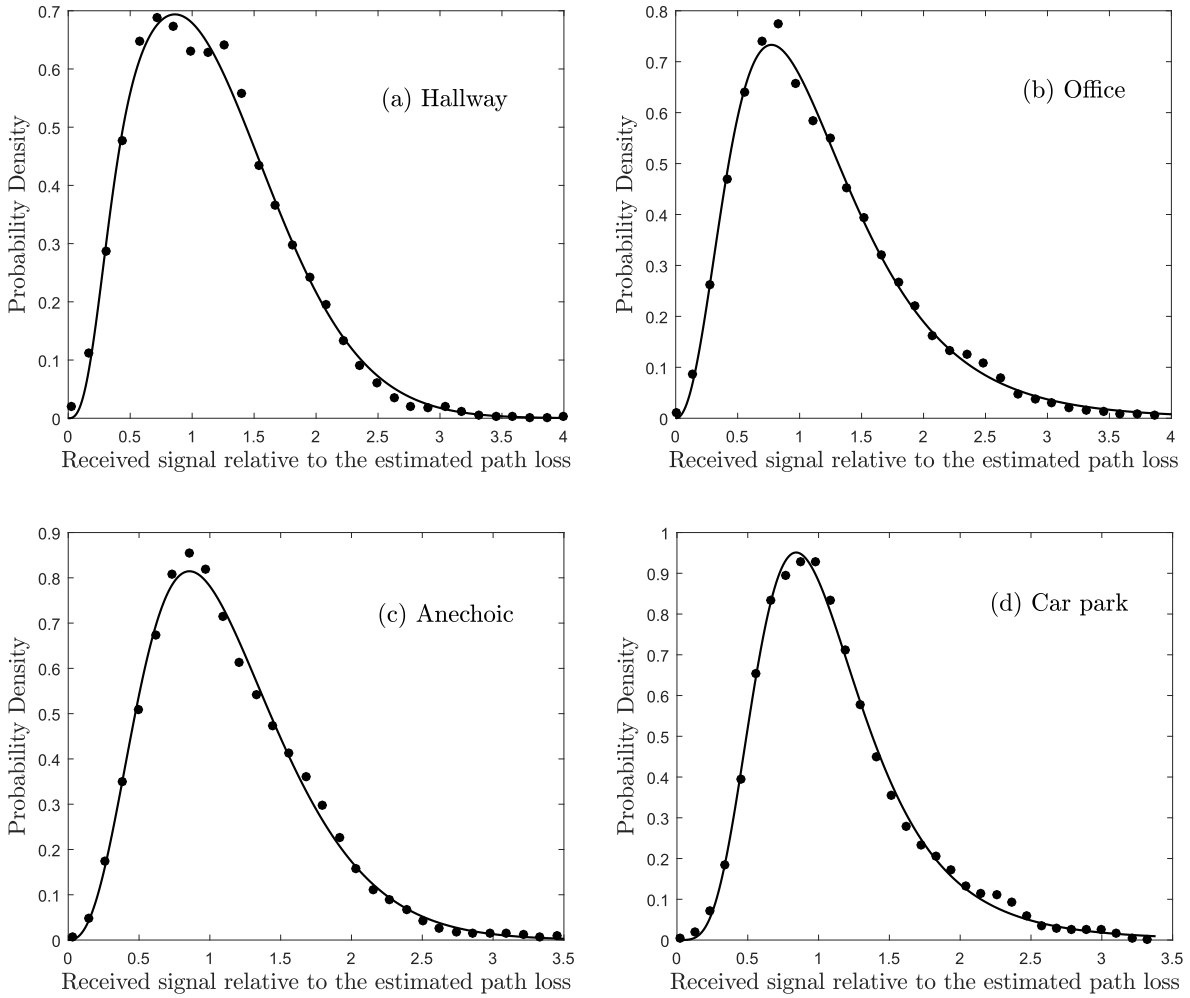

Fig. 4. Empirical PDFs (symbols) of the composite fading observed in the NLOS off-body channel at 60 GHz for (a) the hallway, (b) the open office, (c) the anechoic chamber and (d) the car park environments compared to the theoretical PDFs for the η-μ/inverse gamma (continuous lines) model.

of the in-phase and quadrature components of each cluster of multipath were identical ($\eta = 1$) for the laboratory and open office environments at 5.8 GHz and outdoor car park environment at 60 GHz, but not identical ($\eta \neq 1$) for the remainder of the environments. This suggests that the scattered wave power of in-phase and quadrature components varies according to both the environment and operating frequency. When comparing the μ parameters for the 5.8 GHz and 60 GHz channel measurements, for all of the environments, the μ parameters for the 60 GHz measurements were found to be relatively greater than those for 5.8 GHz, indicating that 60 GHz NLOS off-body channels are more impacted by scattered multipath than 5.8 GHz NLOS off-body channels.

B. Model selection

The Rayleigh and Nakagami-m distributions have been synonymous with small-scale fading in NLOS channel conditions. Furthermore, the Nakagami/gamma model, also known as generalized K (K_G) model, has been proposed based on the Nakagami-m fading model to characterize small-scale fading with shadowing. To ascertain the most probable model among the η-μ/inverse gamma, K_G, Rayleigh and Nakagami-m distributions for characterizing NLOS off-body channels, the Akaike information criterion (AIC) was used. More specifically, we used the second-order AIC (AIC_c) in a similar manner to the analysis employed in [14]

$$AIC_C = -2\ln\left(l\left(\theta|data\right)\right) + 2M + \frac{2M\left(M+1\right)}{n-M-1} \qquad (2)$$

where $\ln\left(l\left(\theta|data\right)\right)$ is the value of the maximized log-likelihood for the unknown parameter θ of the model given the data, M is the number of estimated parameters available in the model, and n is the sample size. It should be noted that the lower the value returned by the AIC_c, then the more likely the candidate model was to have generated the data.

To visually compare the goodness-of-fit of the five candidate models, Fig. 5 shows their PDFs fitted to the NLOS off-body

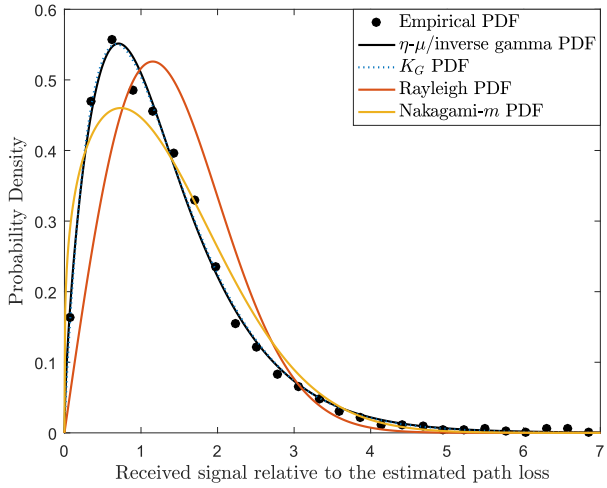

Fig. 5. Comparison of the four candidate fading models for the 5.8 GHz NLOS off-body measurement data in seminar room.

TABLE II
AIC_c RANK FOR ALL OF THE CONSIDERED NLOS OFF-BODY CHANNEL MEASUREMENT DATA.

Frequency	Environments	η-μ/inverse gamma	K_G	Rayleigh	Nakagami-m
5.8 GHz	Laboratory	**1**	2	4	3
	Seminar	**1**	2	4	3
	Open office	**1**	2	4	3
60 GHz	Hallway	**1**	2	4	3
	Open office	**1**	2	3	4
	Anechoic	2	**1**	4	3
	Car park	**1**	2	4	3

measurement data observed in seminar room at 5.8 GHz. It is clear that both of the composite fading models outperformed the Rayleigh and Nakagami-m fading models. Furthermore, as shown in Table II, the five candidate models were ranked according to their AIC_c. It was found that the η-μ/inverse gamma distribution was chosen as the best model for 85.7 % of the cases considered in this study.

V. Conclusion

The characteristics of the composite fading experienced in the NLOS off-body communications channels at 5.8 GHz and 60 GHz have been investigated using the η-μ/inverse gamma distribution. Over all of the channel measurements, the composite fading observed in NLOS off-body channels was well modeled using the η-μ/inverse gamma distribution. Using the AIC_c, it has been shown that the η-μ/inverse gamma composite fading model was selected the best model for the majority of the cases.

Acknowledgment

This work was supported by the U.K. Engineering and Physical Sciences Research Council under Grant Reference EP/L026074/1 and the Department for Employment and Learning Northern Ireland through Grant Reference USI080.

References

[1] A. Abdi, W. C. Lau, M.-S. Alouini, and M. Kaveh, "A new simple model for land mobile satellite channels: first-and second-order statistics," *IEEE Transactions on Wireless Communications*, vol. 2, no. 3, pp. 519–528, May 2003.

[2] H. Suzuki, "A statistical model for urban radio propogation," *IEEE Transactions on Communications*, vol. 25, no. 7, pp. 673–680, Jul. 1977.

[3] A. Abdi and M. Kaveh, "K distribution: An appropriate substitute for Rayleigh-lognormal distribution in fading-shadowing wireless channels," *IET Electronics Letters*, vol. 34, no. 9, pp. 851–852, Apr. 1998.

[4] I. M. Kostić, "Analytical approach to performance analysis for channel subject to shadowing and fading," *IEE Proceedings on Communications*, vol. 152, no. 6, pp. 821–827, Dec. 2005.

[5] S. L. Cotton, "A statistical model for shadowed body-centric communications channels: theory and validation," *IEEE Transactions on Antennas and Propagation*, vol. 62, no. 3, pp. 1416–1424, Mar. 2014.

[6] S. K. Yoo, S. L. Cotton, P. C. Sofotasios, and S. Freear, "Shadowed fading in indoor off-body communication channels: A statistical characterization using the κ-μ/gamma composite fading model," *IEEE Transactions on Wireless Communications*, vol. 115, no. 8, pp. 5231–5244, Aug. 2016.

[7] S. K. Yoo, S. L. Cotton, P. C. Sofotasios, M. Matthaiou, M. Valkama, and G. K. Karagiannidis, "The κ-μ / inverse gamma fading model," in *IEEE Personal, Indoor, and Mobile Radio Communications (PIMRC)*, Sep. 2015, pp. 425–429.

[8] S. K. Yoo, P. C. Sofotasios, S. L. Cotton, M. Matthaiou, M. Valkama, and G. K. Karagiannidis, "The η-μ / inverse gamma composite fading model," in *IEEE Personal, Indoor, and Mobile Radio Communications (PIMRC)*, Sep. 2015, pp. 166–170.

[9] H. R. Chuang, "Human operator coupling effects on radiation characteristics of a portable communication dipole antenna," *IEEE Transactions on Antennas and Propagation*, vol. 42, no. 4, pp. 556–560, Apr. 1994.

[10] A. A. Serra, P. Nepa, G. Manara, and P. Hall, "Diversity measurements for on-body communication systems," *IEEE Antennas Wireless Propagation Letters*, vol. 6, pp. 361–363, Oct. 2007.

[11] M. D. Yacoub, "The κ-μ distribution and the η-μ distribution," *IEEE Antennas and Propagation Magazine*, vol. 49, no. 1, pp. 68–81, Feb. 2007.

[12] S. L. Cotton and W. G. Scanlon, "Characterization and modeling of the indoor radio channel at 868 MHz for a mobile bodywon wireless personal area network," *IEEE Antennas Wireless Propagation Letters*, vol. 6, pp. 51–55, Mar. 2007.

[13] T. S. Rappaport, *Wireless communications: principles and practice*. New Jersey: Prentice Hall PTR, 2002.

[14] A. Fort, C. Desset, P. D. Doncker, P. Wambacq, and L. V. Biesen, "An ultra-wideband body area propagation channel model-from statistics to implementation," *IEEE Transactions on Microwave Theory and Techniques*, vol. 54, no. 4, pp. 1820–1826, Jun. 2006.